Eur. Phys. J. A **25**, 41–47 (2005)
DOI 10.1140/epja/i2005-10064-8

THE EUROPEAN PHYSICAL JOURNAL A

Fission fragment production from uranium carbide disc targets

A. Andrighetto[1,a], S. Cevolani[2], and C. Petrovich[2]

[1] INFN Laboratori Nazionali di Legnaro, Viale dell'Università 2, 35020 Legnaro (PD), Italy
[2] ENEA, Via M.M. Sole 4, 40129 Bologna, Italy

Received: 18 March 2005 /
Published online: 20 June 2005 –
Communicated by C. Signorini

Abstract. A possible solution for a target system aimed at the production of exotic nuclei as a result of high-energy fissions in ^{238}U compounds has been analyzed. The configuration proposed is constituted by a primary proton beam (40 MeV, 0.4 mA) directly impinging on a UC_2 multiple-disc target inserted within a cylindrical tungsten box. In order to extract the fission fragments, the tungsten box has to be kept at 2000 °C. This system has been conceived to obtain both a high number of fission fragments (about $2 \cdot 10^{13}$ atoms/s) and a quite low power deposition in the target. The power release and the fragment distribution have been calculated by means of the Monte Carlo code MCNPX. The thermal analysis of the proposed configuration shows the capability of the thermal radiation to cool the discs with a reasonable margin below the material melting point. Moreover, the possibility of increasing such margin with simple modifications of the target design is shown by means of parametric analyses. The thermal analysis of the tungsten box, also cooled by radiation, points out the necessity to heat it and/or shield it thermally, in order to take it at the requested temperature. Preliminary calculations of the target-induced activity have also been performed.

PACS. 29.25.Rm Sources of radioactive nuclei – 24.10.Lx Monte Carlo simulations (including hadron and parton cascades and string breaking models) – 25.85.Ge Charged-particle-induced fission

1 Introduction

The present study is inserted in the framework of the R&D of the SPES project (Study for the Production of Exotic Species) [1], an accelerator facility providing intense neutron-rich radioactive ion beams of highest quality, in the range of masses between 80 and 160. This can be achieved by means of high-energy fissions in ^{238}U compounds. This facility is planned to be constructed in Italy, at the Legnaro INFN Laboratory (Istituto Nazionale di Fisica Nucleare). The first design project [2] was based on a high-intensity 100 MeV (100 kW) proton LINAC driver; whereas here a configuration with a 40 MeV proton primary beam directly impinging on a multiple-disc uranium carbide target device [3] (ideal UC_2in the present work) is considered as a possible option. The in-target fission fragments and the power deposition are studied by means of the Monte Carlo radiation transport code MCNPX.

The thermal analysis of the proposed system has been performed by considering the discs irradiating towards a tungsten container, to be kept at 2000 °C. The high temperature of the tungsten box is an essential condition for the extraction of the fission products using the ISOL scheme. This is also the reason for the choice of uranium carbide instead of natural uranium as target material. The tungsten box, in turn, is cooled by thermal radiation toward the environment chamber walls, at about room temperature.

Only the in-target isotope production, the activation and the target thermal status are analyzed here, without considering other technological problems (*e.g.* diffusions, effusions, ionisations, etc.). Also the thermo-mechanical analysis of the UCx discs is deferred to a further study.

2 The target configuration

The target configuration has been set considering some main purposes, such as the high number of fission reactions, the fission fragment distribution with a high number of atoms in the whole mass range $80 < A < 160$ and a low power deposition in the materials (both window and target). The most exploited solution in the RIB projects is the 2-step configuration [4], consisting of a proton/deuteron beam impinging on a converter target used to emit fast neutrons for fissioning the uranium target. On the other hand, the 1-step target configuration is chosen here, consisting of a proton beam directly impinging

[a] e-mail: alberto.andrighetto@lnl.infn.it

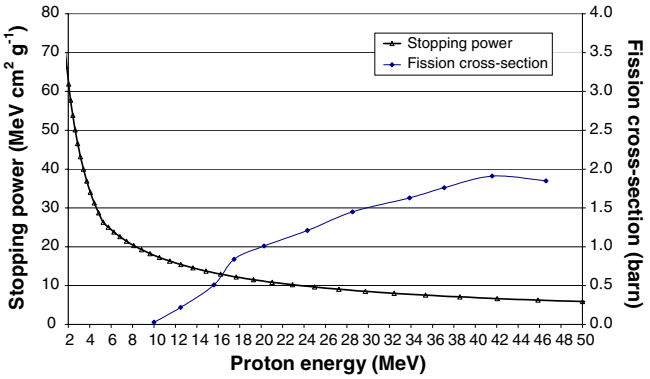

Fig. 1. Stopping power and fission cross-section for protons on UC_2.

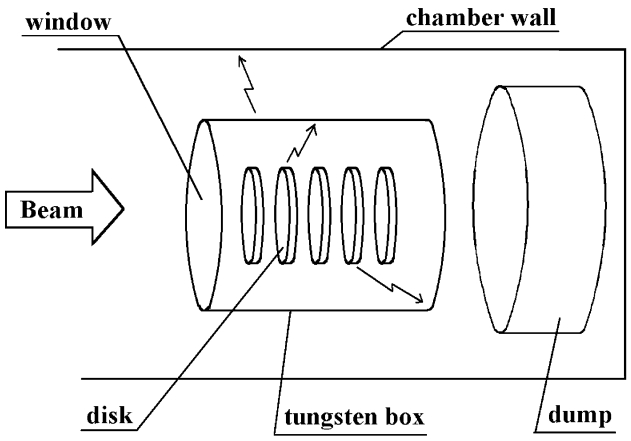

Fig. 2. Configuration 1-step with the multiple-disc target.

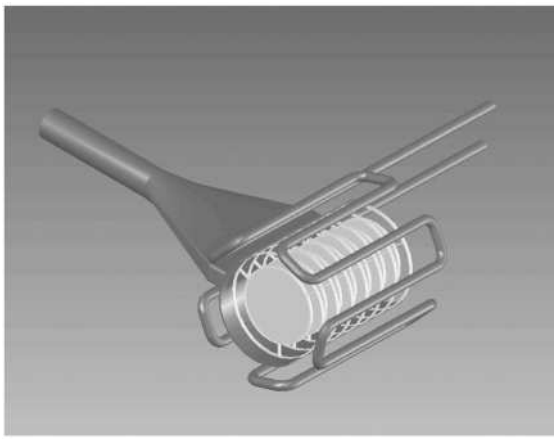

Fig. 3. Preliminary layout of the target prototype.

on the fission target [5]. The main problem of the 1-step configuration concerns the high power deposition of the incident beam in the production target, mainly due to the electromagnetic interactions. However, a solution to this drawback has been conceived: only the protons with higher fission cross-section are exploited in a thin target, while the outgoing lower-energy beam is driven towards a passive dump. As a matter of fact, the ^{238}U fission cross-section and the stopping power have opposite dependency on the proton energy, as shown in fig. 1 [6–8]. It is clear that low-energy protons (for example, with energy lower than 25 MeV) are less efficient for a production target, having lower fission cross-section and higher stopping power values. For this reason they have been chosen to be driven towards a passive dump. In this way the power deposited in the target is lowered considerably and at the same time the number of fission reactions is kept high.

As far as the choice of the energy of the primary proton beam is concerned, it has to be noticed that even if high-energy protons involve less dissipated energy per length and a longer range, they increase sensitively the cost of the apparatus. Moreover, the ^{238}U fission cross-section does not increase considerably for energies higher than 40 MeV (as shown in fig. 1). This is the value that has been chosen for the primary proton beam.

In order to optimize the heat dissipation, a good solution is the use of a target constituted by multiple discs. In this way the cooling of the target is strongly simplified: in fact, due to the void environment, the heat dissipation is fully entrusted to the thermal radiation and this mechanism is directly proportional to the body surface. The use of several thin discs, the mass being equal, increases the total surface and allows for better cooling.

All these considerations lead to the system configuration shown in fig. 2 and fig. 3: the target itself is constituted by several discs about 1 mm thick, preceded by a thin window (necessary to separate the beam line with the target void regions) and followed by a carbon dump, in which the protons with low production rate and high stopping power are driven.

In this study, the number of the discs has been chosen to be 5. The material of the discs is pure UC_2 of density 2.5 g/cm^3, leading to a total mass of about 40 g. The discs have a radius of 3 cm and thicknesses varying from 1.3 mm down to 0.9 mm. In order to optimize the power deposition, the thicknesses of the discs have decreasing values as a compensation of the increasing values of the stopping energy per length. The thicknesses are also a compromise between the need of low-energy deposition (thinner targets are preferred) and mechanical resistance of the material (thicker targets are preferred). The window is constituted by a thin tungsten foil of 100 μm.

3 Calculations of the power deposition and of the in-target isotope production

The fundamental parameters of the target system, that is the fission rate, the fission fragment distribution and the power deposition, have been calculated by means of the Monte Carlo radiation transport code MCNPX. The code is briefly described and discussed in the following section.

3.1 The MCNPX code

MCNPX [9] (version 2.5.e) allows a detailed 3D definition of the system to be analyzed and a full transport

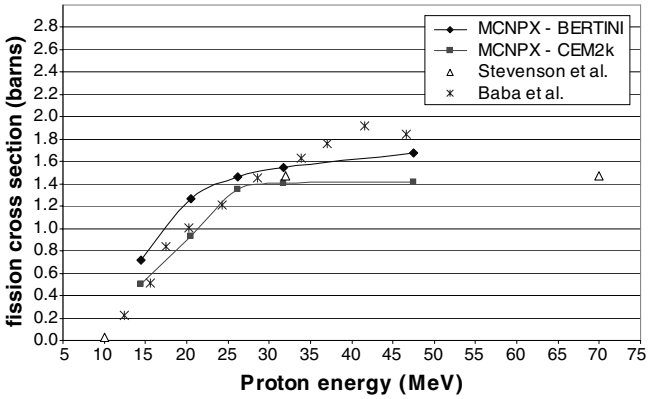

Fig. 4. Comparison of experimental and calculated ^{238}U proton fission cross-sections.

calculation, starting from the proton particles. The interaction physics in MCNPX is determined in two ways: through table-based cross-section data and through online calculations by means of physics models. For neutrons below 20 MeV, the nuclear reactions are taken into account by means of cross-section evaluations (such as ENDF/B-VI). Whenever evaluated cross-section libraries are missing, MCNPX offers different physics models describing the nuclear interactions by the transition of different stages: in the first stage the incident particle interacts with the individual nucleons of the nucleus via particle-particle cross-sections emitting high-energy particles and light ions. This phase is called Intra-Nuclear Cascade (INC) and is followed by a pre-equilibrium stage. In the second stage, the residual nucleus either undergoes evaporation, releasing neutrons and light ions, or fissions. In the final stage the excited nucleus decays by gamma emission. Among these physics models there are the Bertini-Dresner Model [10] and the CEM2k (Cascade-Exciton-Model) [11]. The fission model used to describe the fragmentation distribution is the RAL (Rutherford Appleton Laboratory) fission model [12]. The fission yields are finally obtained by means of the HTAPE3X code [9].

Since evaluated cross-section data for protons interacting with ^{238}U are missing (the most important interaction for this target system), a validation of the fission process described by the above-mentioned models has been performed. The proton fission cross-sections obtained by means of MCNPX calculations using the Bertini model and the CEM2k model have been compared with the experimental data found in the literature [6,7] (see fig. 4). CEM2k is in good agreement (discrepancies below 15%) with the data of [6] in the whole energy range. It has some discrepancies (up to 35%) with the data of [7] in the range 35–50 MeV. The Bertini model has discrepancies with the experimental data and with CEM2k in the range 10%–35%. These comparisons are considered here to be good enough for an analysis of the target system by means of MCNPX. The Bertini model has been chosen for these calculations.

Table 1. Thicknesses and power deposition in the target discs.

	Target # 1	Target # 2	Target # 3	Target # 4	Target # 5
Thickness (mm)	1.3	1.2	1.1	1.0	0.9
Power (kW)	0.74	0.71	0.70	0.65	0.63

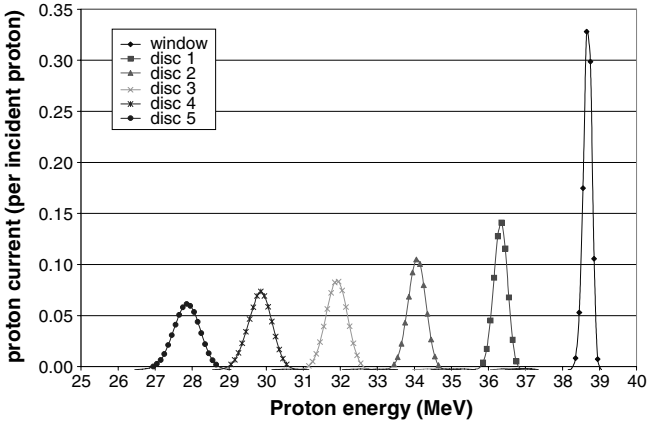

Fig. 5. Energy of the proton beam coming out of the target discs.

3.2 Results of the Monte Carlo calculations

The Monte Carlo calculations were performed modeling the 40 MeV proton beam as a Gaussian shape and the target configuration as described previously. The results, using a proton current of 0.4 mA, show that a power of 0.4 kW is deposited in the window, 3.4 kW in all the target discs, and most of the beam power is driven into the dump (about 12 kW). The power deposition in each target disc is shown in table 1 and the average value is about 0.7 kW. This corresponds to a power density averaged in the whole UC_2 target mass of less than 100 W/g.

Preliminary calculations, reported in the next section, show that these values do not represent a serious problem for the target, because the mean temperature remains below the UC_2 melting point if an appropriate target disc radius is used.

The energy distribution of the protons coming out of the target discs is shown in fig. 5. The proton beam impinges on the first disc at about 39 MeV and leaves the last disc with an energy of about 28 MeV.

The calculated fission rate in all the 5 discs turns out to be about $9 \cdot 10^{12}$ fissions per second ($1.8 \cdot 10^{13}$ atoms per second are thus produced). Obviously they are not uniformly distributed in the 5 discs because of the decrease of the disc thickness and of the beam energy: the fission reactions in the last disc are 40% less than those of the first disc. The fission reactions due to neutrons have also been calculated but turn out to be negligible ($< 1\%$) with respect to those induced by protons.

The distribution of the fission products for the mass numbers $70 < A < 170$ is shown in fig. 6. It can be

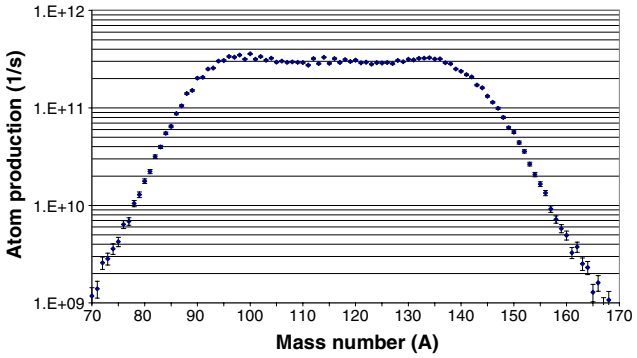

Fig. 6. Fission mass spectra yields.

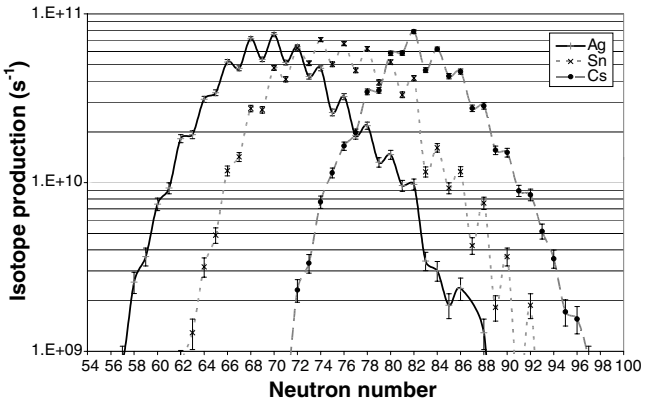

Fig. 7. In-target isotope distribution for silver, tin and caesium.

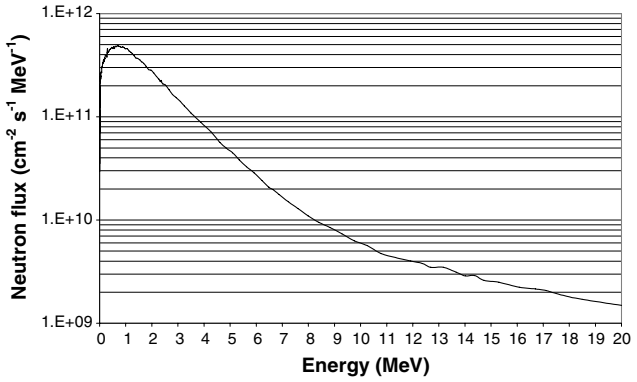

Fig. 8. Average neutron flux in the target discs.

noticed here that the local minimum that is present in thermal-neutron–induced fissions at about $A = 115$–120 is almost absent. This was an intended result since the RIB to be produced lie in the mass range $80 < A < 160$. The isotope production distribution for some interesting atoms (Ag, Sn, Cs) is shown in fig. 7, reaching values up to $8 \cdot 10^{10}$ atoms/s. However, it should be remarked that the neutron-rich and the neutron-deficient sides are overpredicted by the RAL fission fragmentation model.

The neutron numbers corresponding to the peaks (fig. 7) are quite close to those obtained in the case of the 2-step configuration, where the fission reactions are induced by neutrons [2].

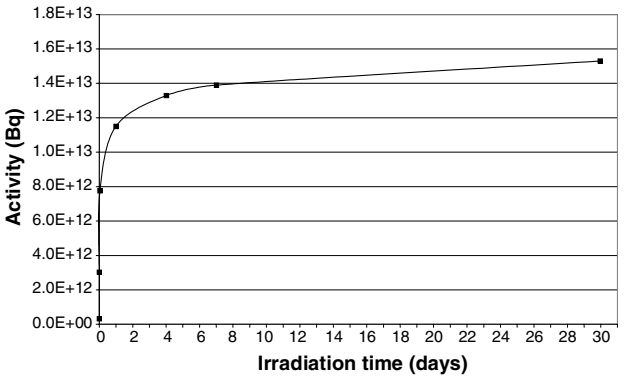

Fig. 9. Accumulation of the target-induced activity during a full irradiation time of 1 month (tritium activity not included).

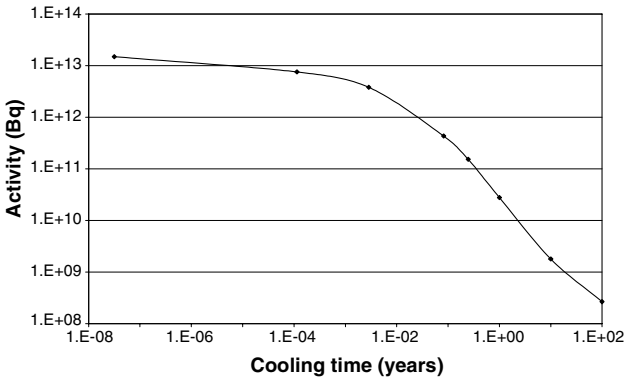

Fig. 10. Cooling behaviour after an irradiation of 1 month (tritium activity not included).

Another parameter that has been calculated is the activity induced in the discs. Of course the activity is mainly due to the proton fission reactions, but also the contribution from the neutron flux (the average value being $1.3 \cdot 10^{12}\,\mathrm{cm}^{-2}\mathrm{s}^{-1}$) has been evaluated. This is shown in fig. 8, where the peak at about 1 MeV corresponds to the typical energies of the evaporation stage.

The activity calculations have been performed by means of the activation code SP-FISPACT [13], which is a modified version of the FISPACT code [14] to calculate the accumulations and decays of the fission products provided by MCNPX. With a proton current of 0.4 mA and a full irradiation time of 1 month the activity turns out to be of the order of $1 \cdot 10^{13}$ Bq (after 1 hour of irradiation the value is already $8 \cdot 10^{12}$ Bq). The behaviour of the activity during the irradiation time and the cooling time are shown, respectively, in fig. 9 and fig. 10. It has to be pointed out that this represents only a rough estimation since about 1/3 of the on-target isotopes are not taken into account in the activity calculation (the decay data of such exotic nuclei are not included in the FISPACT data library) and the impact of such an approximation is not clearly assessable.

The summary characteristics of the system configuration analyzed are shown in table 2. The ^{132}Sn isotope yield is also reported because, being a double magic nucleus, it is one of the interesting radioactive nuclei to be produced.

Table 2. Summary table.

Beam energy (MeV)	Beam current (mA)	UC_2 mass (g)	Power in UC_2 (kW)	Atoms produced (s^{-1})	^{132}Sn (s^{-1})
40	0.4	40	3.4	$2 \cdot 10^{13}$	$\sim 10^{10}$

The results obtained show the promising features of the target configuration proposed. A first necessary verification for the system feasibility is constituted by the thermal status of the discs and of the tungsten box.

4 Target thermal analysis

In order to discuss the problems concerned with the thermal analysis of the target proposed, the scheme shown in fig. 2 is taken as reference.

The energy deposited in the discs by the beam-target interaction has to be removed. Due to the low pressure of the target environment, the discs can be only cooled by thermal radiation towards the tungsten box surrounding them; for the moment, this box is assumed to have a cylindrical shape. In turn, the tungsten box will transfer heat, also by radiation, toward the walls of the chamber where the target is placed. The final cooling of the chamber walls will not be taken into account in the present analysis: probably, the natural convection with the air of the building will be sufficient for this purpose; but in any case the adoption of a water cooling system will not be a problem. As a consequence, the chamber wall temperature will be assumed here to be constant, uniform and equal to a reference value of 50 °C, close to room temperature.

Then the heat transfer phenomena to be analysed are two: the first one takes place between the discs and the box inner surface, whereas the second one acts between the box outer surface and the chamber walls. In both cases, a singular feature has to be taken into account, *i.e.* the fact that the tungsten cylinder has to be kept at about 2000 °C.

With respect to the discs, the tungsten box acts as heat well and, being at a temperature so high, the coolability of the discs is not obvious: the melting point of their material is in fact about 2350 °C (a fair average between [15] and [16]).

With respect to the box, the radiation heat transfer at such high temperature will be surely very effective; as a consequence, it may become greater than the power transmitted to the box by the discs. Then it is possible that the box does not have to be cooled, but heated up.

4.1 Disc thermal analysis

The complexity of the study of the radiation heat transfer depends on the number of bodies to be considered and on the temperature distribution on the surface of each body. If a single body at uniform surface temperature is transferring heat towards an enclosure also at uniform temperature, the task is very simple. If the temperature of the body is not uniform, for example if the heat generation within it is not uniform, the problem becomes more complicated but can be faced by solving the Fourier equation for thermal conduction inside the body linked with a boundary condition of thermal radiation. If the enclosure contains several bodies each of them at uniform surface temperature, the analysis of the radiation mechanism becomes even more complicated, but still manageable. But when several bodies are involved and their surface temperature cannot be assumed as uniform, the problem becomes very complex, as in the present case.

In order to face a similar situation, in [17] a simplified procedure was adopted. It is based on the use of two computer models, each of them facing one of the complications mentioned. The first model (called here *multi-disc model*) takes into account all bodies, but by considering them at a uniform surface temperature. The second one (the *single-disc model*) performs the analysis of a single body, but by taking into account the actual power distribution, *i.e.* the actual temperature distribution at the surface. Then the final temperature distribution is obtained by superposing the results of the two models. This procedure will also be adopted here.

The disc geometry is the one presented in sect. 2; the distance between adjacent discs is a (relatively) free parameter, to be determined also by the thermal-analysis results (see sect. 4.1.2). The form and the dimensions of the tungsten box are also (relatively) free; in the following, the cylindrical shape was taken as reference. As for the dimensions, the cylinder height was taken equal to six times the distance between the discs (see later); the diameter was fixed at 100 mm, slightly greater than the disc diameter; but it has to be pointed out that the cylinder diameter has little impact on the disc thermal status.

The power deposition data used for the analysis are those presented in table 1. In this preliminary stage, the Gaussian standard deviation = 20 mm of the beam in the radial direction was assumed as representative of the radial power distribution in all discs. In the beam direction, the power deposition inside a disc is slightly decreasing but, for the moment, it was assumed to be uniform. Finally, in the azimuthal direction, the power deposition can be reasonably assumed to be uniform.

The disc material physical properties of interest at the working temperature foreseen were taken from [18]: the thermal conductivity was assumed to be $1.0\,W\,m^{-1}\,°C^{-1}$ and the total emissivity equal to 0.60.

In all the performed calculations the tungsten box was assumed to be at a uniform surface temperature equal to 2000 °C.

4.1.1 Reference case

For this case, actually the first guess case, the distance between the discs was assumed to be equal to 20 mm. By using the above-mentioned procedure, the results presented in table 3 were obtained.

The most important result is that the maximum temperature (about 2300 °C) is lower than the melting point.

Table 3. Temperatures of the discs resulting from the superposition.

Hottest disc (number, from left)	–	3
Hottest-disc average surface temperature	°C	2190
Hottest-disc average mid-plane temperature	°C	2224
Hottest-disc average surface-center ΔT	°C	34
Hottest-disc max surface temperature	°C	2236
Hottest-disc max mid-plane temperature	°C	2303
Materials melting point	°C	2350
Hottest-disc max surface-center ΔT	°C	67
Hottest-disc min surface temperature	°C	2158
Hottest-disc max surface radial ΔT	°C	78

The margin is small, but in the present conditions it cannot be much higher. Anyway, a design effort to increase the margin to avoid melting is opportune and was performed, as shown in the following section.

Further interesting results are constituted by the ΔT's, providing a measure of the thermal gradients in the disc.

4.1.2 Parameterizations

As shown in the previous section, the reference target design seems to be feasible with respect to the target material melting point, but with a small margin.

At fixed deposited power, a first possibility in order to increase this margin, *i.e.* in order to decrease the target material temperature, is concerned with the increase of the distance between the discs. The discs are in fact hotter than the cylinder: to increase that distance improves the heat transmission between the disc and the cylinder and consequently leads to lower disc temperatures.

A parametric analysis of this effect was performed by means of the *multi-disc model*, considered sufficient for comparison purposes. Actually, for any new value of this distance, the power distribution analysis should be repeated; on the contrary, in the calculations performed, only the distance was changed. Then, the results obtained are significant only for the comparison, not as absolute values; and particularly, they are not comparable with those presented in the previous section.

The results obtained are shown in fig. 11, where the maximum surface and mid-plane temperatures in the hottest disc (disc No. 3) are plotted *versus* the distance between the discs.

It appears that the increase of the disc distance is a very effective tool for decreasing the disc temperature. Moreover, fig. 11 shows that, in the examined range of distances, the curve is still far from an asymptotic behaviour: the analysis was in fact stopped at a disc distance giving a very reasonable increment in the cylinder size. This limitation is due to the fact that the present analysis does not take into account any physical consideration concerned with the disc distance increase. The determination of the allowable maximum cylinder size is devoted to a further work.

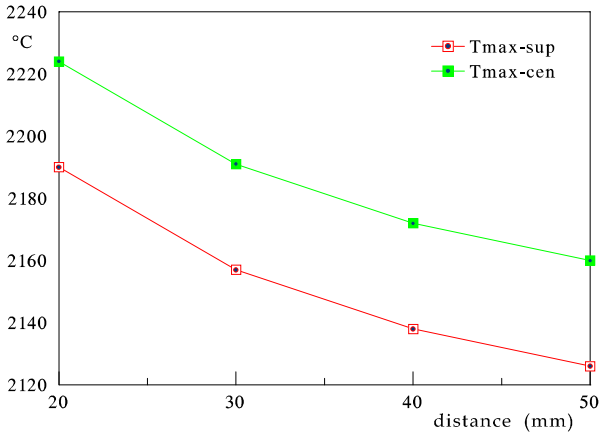

Fig. 11. Parameterization of the distance between the discs (sup = disc surface; cen = disc centre).

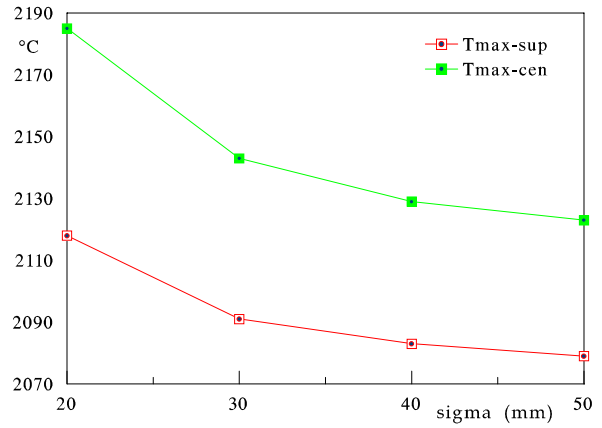

Fig. 12. Parameterization of the beam sigma (sup = disc surface; cen = disc centre).

A further way to decrease the disc temperatures can be the flattening of the power deposition profile. As mentioned above, the reference calculation was based on a 20 mm sigma Gaussian profile of the beam. A flatter distribution can be obtained either by increasing the sigma (by constant total power) or by moving rapidly a small beam all over the disc surface. In the following analysis only the effect of the beam sigma increase is considered.

As in the former parameterization, the calculations were performed by changing only this parameter and by using the *single-disc model*: again the results obtained are sufficiently accurate for the sake of comparison but they should not be taken as absolute values and are not comparable with the data presented in sect. 4.1.1.

The effect of the beam sigma is presented in fig. 12, where the surface and mid-plane temperatures of disc No. 3 are plotted *versus* the sigma.

As expected, also the beam sigma appears to be an effective tool for reducing the disc temperature. Anyway, in this case the curves are closer to their asymptotic value than in the previous one.

As a conclusion, both these simple possibilities showed to be able to reduce significantly the temperature of the discs.

4.2 Box thermal analysis

Quite surely, the surface temperature distribution in the tungsten box will not be uniform; this should be taken into account in a careful study of the box thermal status. But the main interest at the moment is devoted to the global box behaviour and, for this purpose, the surface temperature can reasonably be assumed to be uniform. In such conditions, that is a single body (the box) inside a uniform temperature enclosure (the chamber walls), the analysis is very simple. For such purpose, the only physical property of interest is the tungsten global emissivity: the emissivity of the low-temperature chamber walls is in fact quite negligible. Such property is very well known and, at 2000 °C, it turns out to be equal to 0.25 [19].

In this analysis, the temperatures of the cylinder and of the chamber walls are imposed: the result is the heat transmitted from the box to the chamber. It turns out that the power necessary to keep such a situation is about 20 kW. Due to the fact that the total power deposited in or transmitted to the cylinder is about 4 kW (table 1), it follows that the cylinder has to be continuously heated with about 15 kW.

The former analysis is approximate but it demonstrates that the cylinder has to be heated and gives a reasonable evaluation of the power necessary for this purpose.

It has to be pointed out that, in order to keep the box itself at 2000 °C, the heating of the box is not strictly necessary: an equivalent effect could be obtained by inserting some insulation layer between the box and the chamber walls.

5 Conclusions

A possible solution for producing exotic nuclei is a configuration with a proton beam of 40 MeV and a current of about 0.4 mA impinging directly on a multiple-thin-disc UC_2 target. In this way about $2 \cdot 10^{13}$ s^{-1} fission residuals are formed as a result of high-energy fissions in ^{238}U compounds. The fission fragment distribution has been calculated by means of the MCNPX code, here validated as far as the fission cross-section is concerned. Preliminary numerical calculations suggest that the power deposited by the beam in the production target (about 3.4 kW), might not represent a critical engineering issue. In fact, the thermal analysis shows the capability of the thermal radiation to cool the discs with a reasonable margin to the material melting point. Moreover, the possibility of increasing such margin with simple modifications of the target design is shown by means of parametric analyses. The thermal analysis of the tungsten box, also cooled by radiation, shows the necessity to heat it and/or insulate it, in order to take it at the temperature requested.

In any case, further and detailed R& D study on the isotopes release behaviour of the uranium carbide target is required to demonstrate the feasibility of the whole system.

We wish to thank A. Pisent, G. Cuttone, G. Fortuna, M. Lollo, M. Menna, M. Re and R. Tinti for their precious collaboration and helpful discussions.

References

1. A. Bracco, A. Pisent (Editors), *SPES Technical Design for an Advanced Exotic Ion Beam Facility at LNL*, (REP)181/02 (LNL-INFN, 2002).
2. A. Andrighetto, J. Li, C. Petrovich, Q. You, Nucl. Instrum. Methods B **204**, 205 (2003).
3. E.K. Storms, *The Refractory Carbides* (Academic Press, New York, London, 1967).
4. M. Mirea *et al.*, Eur. Phys. J. A **11**, 59 (2001).
5. A. Andrighetto, *Proceedings of Exon 2004 Internatioal Conference* (World Scientific Publishing Company, 2004).
6. P.C. Stevenson *et al.*, Phys. Rev. **111**, 886 (1958).
7. S. Baba *et al.*, Nucl. Phys. A **175**, 177 (1971).
8. B.L. Tracy *et al.*, Phys. Rev. C **5**, 222 (1972).
9. J.S. Hendricks *et al.*, *MCNPX, Version 2.5.e*, LA-UR-04-0569 (2004).
10. H.W. Bertini, Phys. Rev. **131**, 1801 (1963).
11. S.G. Mashnik, A.J. Sierk, J. Nucl. Sci. Technol. Suppl. **2**, 720 (2002).
12. F. Atchison, *Spallation and fission in heavy metal nuclei under medium energy proton bombardment*, in *Targets for Neutron Beam Spallation Sources*, Jül-Conf-34, Kernforschungsanlage Jülich GmbH (1980).
13. C. Petrovich, *SP-FISPACT2001 A Computer Code for Activation and Decay Calculations for Intermediate Energies. A Connection of FISPACT with MCNPX*, RT/ERG/2001/10 (ENEA, 2001).
14. R.A. Forrest, *FISPACT-2001: User Manual* (UKAEA FUS 450, 2001).
15. M.M. El-Wakil, *Nuclear Power Engineering* (McGraw-Hill, 1962).
16. S. McLain, J.H. Martens (Editors), *Reactor Handbook* (Interscience Publishers, 1964).
17. S. Cevolani, *Valutazioni termiche su un Multifoil target per TRADE*, FIS.P99R.003 (ENEA, 2004).
18. J.A. Nolen, M. Petra, J. Green, *Thermal Conductivity Measurements of Porous Materials at High Temperatures* (R&D Related to a Future Rare Isotope Accelerator Facility).
19. R.C. Weast (Editor), *Handbook of Chemistry and Physics*, 56th edition (CRC Press, 1976).